Available online at www.sciencedirect.com

ScienceDirect

Ceramics International 39 (2013) 8341–8346

CERAMICS INTERNATIONAL

www.elsevier.com/locate/ceramint

Mode I fracture toughness of short carbon fiber-dispersed SiC matrix composite fabricated by melt infiltration process ☆

R. Inoue[a], J.M. Yang[a,b], H. Kakisawa[a], Y. Kagawa[a,c,*]

[a]Research Center for Advanced Science and Technology (RCAST), The University of Tokyo, 4-6-1 Komaba, Meguro-ku, Tokyo 153-8904, Japan

[b]Department of Materials Science and Engineering, University of California, Los Angeles, CA 90095-1595, USA

[c]Composite Materials Group, Hybrid Materials Center, National Institute for Materials Science (NIMS), 1-2-1, Sengen, Tsukuba, Ibaraki 305-0047, Japan

Received 20 January 2013; received in revised form 31 March 2013; accepted 4 April 2013
Available online 19 April 2013

Abstract

Measurement of mode I fracture toughness of in-plane random oriented short carbon fiber-dispersed SiC matrix composite fabricated by melt infiltration process has been carried out. Fracture toughness (K_{Ic}) measured using a Brazilian disk specimen is $\sim$3.5–4.1 MPa$\sqrt{m}$, which is comparable to those of monolithic engineering ceramics. The measured toughness is explained using average stress and characteristic length (χ_D) of damage zone formed ahead of notch tip: $K_{Ic} \approx \sigma_F \sqrt{\pi \chi_D / 2}$. Crack arrest behaviors in the short carbon fiber-dispersed SiC mini-composite play an important role on the stability of micro-cracks in the damage zone before unstable crack growth.

Keywords: B. Composite; C. Toughness; Carbon fiber; SiC matrix; Criterion

1. Introduction

Short carbon fiber-dispersed SiC matrix (hereafter denoted as SCF/SiC) composites fabricated by Si melt infiltration (MI) process have been used for light-weight tribological applications, such as brake disks and pads, clutch for high performance cars, emergency brake disks for high speed transportation trains, etc. [1–5]. These applications become possible because usually SCF/SiC composites behave as extremely tough materials, which allows safety application of the composite under extremely severe environment.

It has been known that addition of short fibers to a ceramic material improves fracture toughness of ceramics and the effect has been reported in various kinds of fiber–matrix combinations [6,7]. Major toughening mechanisms for these short fiber-dispersed ceramic matrix composites are fiber bridging, crack deflection, microcracking, etc. In the case of SCF/SiC composites, some mechanical properties of the composites, such as Young's modulus, tensile/flexural strength, etc., have been reported [1–5]. However, only limited studies are available on measurement of fracture toughness of short carbon fiber-dispersed SiC matrix composite fabricated by MI process.

In the present study, fracture toughness tests of SCF/SiC composites have been carried out using a Brazilian disk specimen. Measured mode I fracture toughness of the composite is discussed in terms of fracture process.

2. Experimental procedure

SCF/SiC composite fabricated by Si melt infiltration (MI) process was used in this work. Processing procedure is similar to conventional MI process published in the available literature [1–5,8,9]. An as-fabricated composite disk with a diameter of 50 mm was supplied by Covalent Material Co. Ltd., Tokyo, Japan. Pitch-based short carbon fibers (DIALEAD®,

*Corresponding author at: Research Center for Advanced Science and Technology (RCAST), The University of Tokyo, 4-6-1 Komaba, Meguro-ku, Tokyo 153-8904, Japan. Tel.: +81 3 5452 5086; fax: +81 3 5452 5087.
E-mail address: kagawa@rcast.u-tokyo.ac.jp (Y. Kagawa).

0272-8842/$ - see front matter © 2013 The Authors. Published by Elsevier Ltd. All rights reserved.
http://dx.doi.org/10.1016/j.ceramint.2013.04.014

K223HG) from Mitsubishi Plastics Inc. (Tokyo, Japan) were dispersed in SiC and Si phases. Each carbon fiber bundle contains 12,000 fibers. The carbon fiber has a Young's modulus of 900 GPa, and a tensile strength of 3.8 GPa. Fig. 1(a) and (b) shows a typical example of the microstructure of SCF/SiC composite both in-plane and through-the-thickness planes. Fig. 1(c) shows typical example of polished in-plane section. Fiber bundles are randomly distributed in the SiC matrix. Within each fiber bundle, individual carbon fiber is surrounded by SiC matrix; hence, it is referred to as a "SCF/SiC mini-composite". Cracks exist in the polished sections, which are formed during processing of the composite (see Fig. 1(d) and (e)). Most of the cracks are located in the SiC matrix; these results are consistent with the previous reports on a similar kind of composites [4]. X-ray diffraction analysis confirmed that this composite is composed of carbon, silicon, α-SiC and β-SiC. It is difficult to distinguish polytypes of SiC within the present analysis; therefore both SiC phases are named as "SiC phase." The measured average length of the fiber (L_f) in the bundle of SCF/SiC mini-composite is ~4 mm.

Distribution of fiber bundle orientation in-plane section and through-the-thickness section obtained by image analysis is shown in Fig. 2. The distribution of the fiber axis observed in in-plane section seems random. However, distribution of fiber axis in through-the-thickness direction appears to be parallel to the in-plane direction. These results indicate that the distribution of SCF/SiC mini-composite has in-plane random orientation.

Volume fractions are measured using image analysis of the polished sections of the composite. Micrographs taken by optical microscopy with a typical magnification of 5× are used for the image analysis. The fiber volume fraction (c_f: $0 < c_f < 1$) of the composite is measured to be c_f ~0.3.

The density of composite was measured by the Archimedes method to be ~2.7 g/cm^3. Selected typical mechanical properties of the composite are presented in Table 1.

Fig. 3 shows shape and dimensions of specimen and schematic drawing of test procedure. Definition of *X–Y–Z* coordinates and applied compressive load direction are also shown in the figure. The diameter of the disk specimen (2*R*)

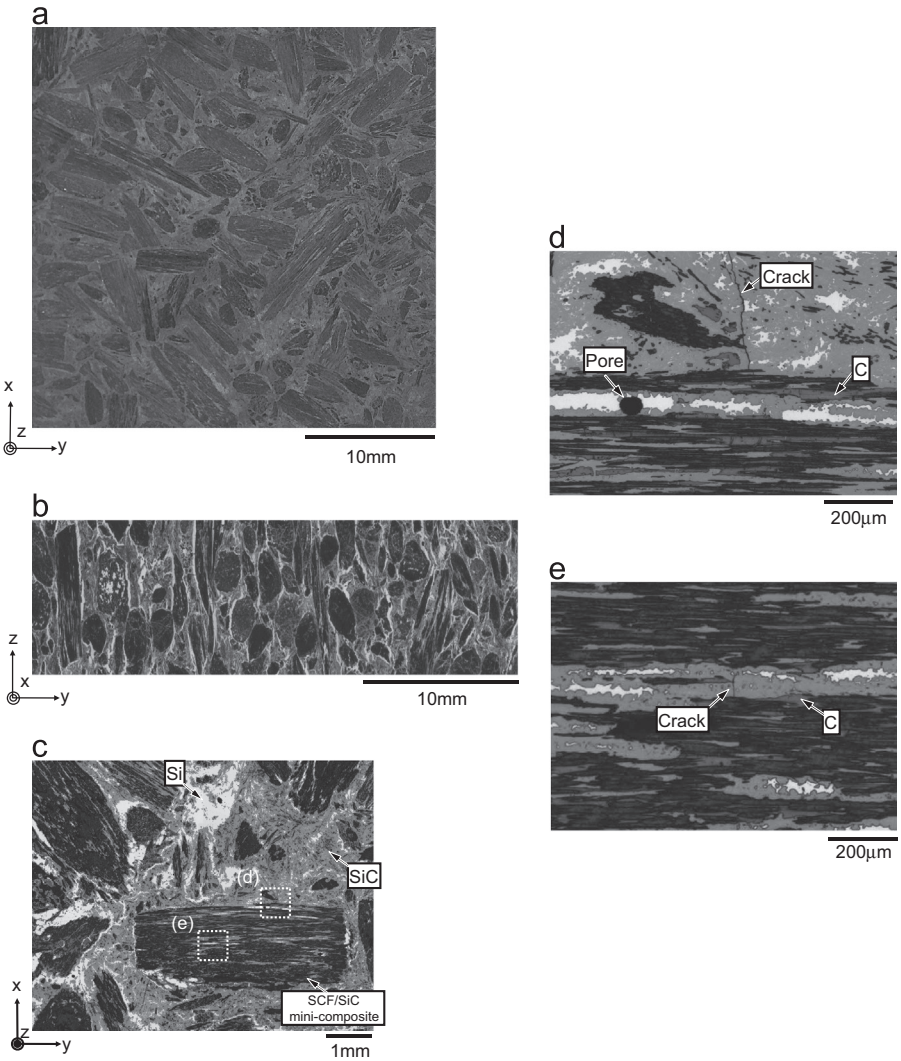

Fig. 1. Typical appearances of SCF/SiC composite in (a) in plane section and (b) through-the-thickness section. (c)–(e) Typical polished surface in plane section.

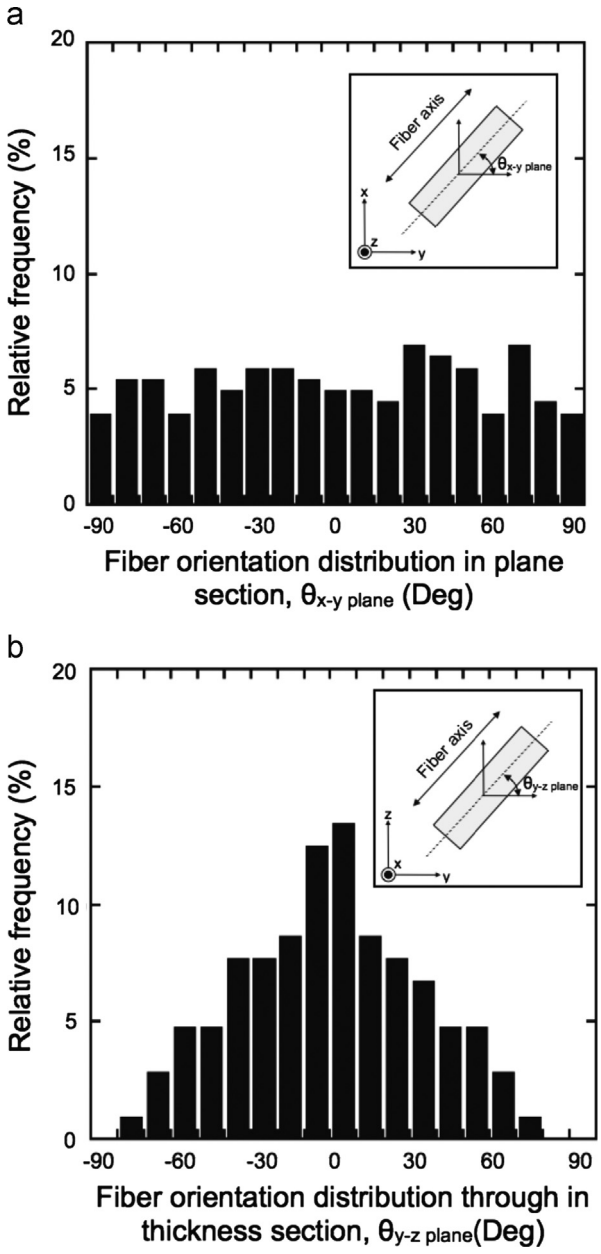

Fig. 2. Distribution of fiber-bundle orientation: (a) in-plane and (b) through-the-thickness plane.

Table 1
Some mechanical properties of SCF/SiC composite.

Properties	
Density (g/cm^3)	2.4–3.0
Tensile Young's modulus (GPa)	5–10
Compressive Young's modulus (MPa)	70–80 (in-plane) 50–55 (out-of-plane)
Tensile strength (MPa)	35–55
Compressive strength (MPa)	210–240 (in-plane) 180–205 (out-of-plane)

was 50 mm with a thickness (t) of 3 mm. Straight notch was introduced to as-fabricated SCF/SiC disk-shape specimen using an arc-discharge machining process. The width of notch

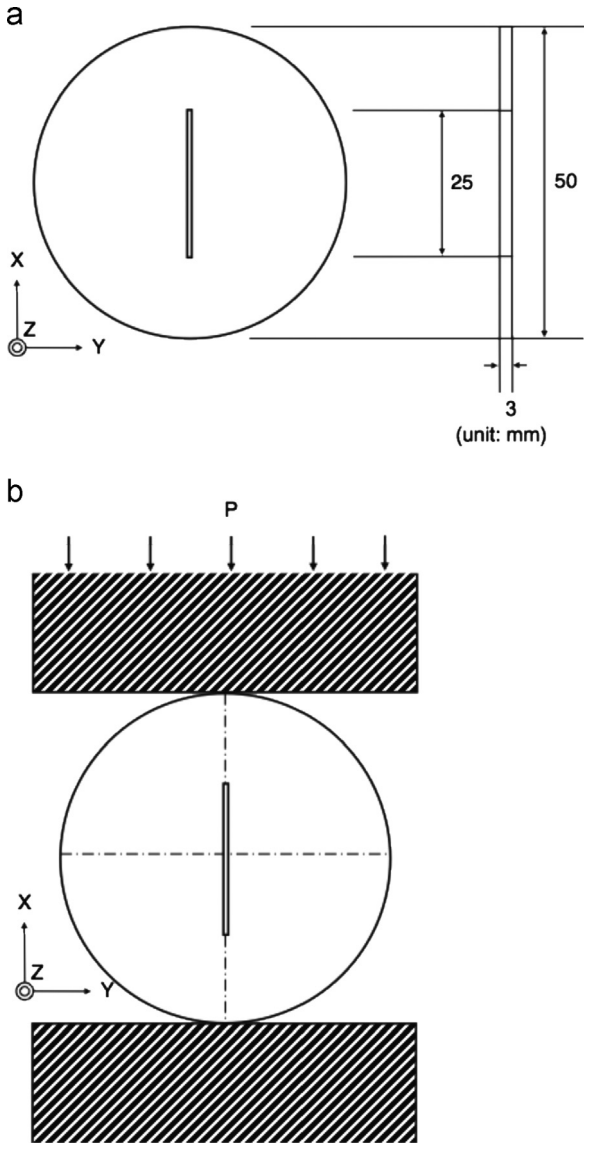

Fig. 3. (a) Shape and dimensions of Brazilian disk specimen and (b) schematic drawing of loading procedure.

was ~100 μm and the tip radius was ~75 μm. Initial notch length ($2a_0$) was 25 mm and this geometry yields $a_0/R \approx 0.5$. Flat surfaces of the specimen were carefully polished through a standard metallurgical procedure up to 0.5 μm diamond paste finish. This surface finish was enough to observe damage evolution behavior at the surface.

Fracture toughness tests were carried out under various loading conditions: notch direction was set parallel to the Y-axis (mode I loading). The disk specimen was sandwiched between hard sintered SiC plates with a Young's modulus ≈400 GPa. Care was taken to adjust notch direction and loading direction. The notch direction was set parallel to loading direction within an error of ≈0.5°. Compressive load was applied to the specimen using an Instron-type test machine (maximum capacity 50 kN, Model 4204, Instron Corp., MA, USA). The fracture tests were done in ambient air condition (20 °C) with a constant crosshead displacement rate of 50(10^{-5} m/s).

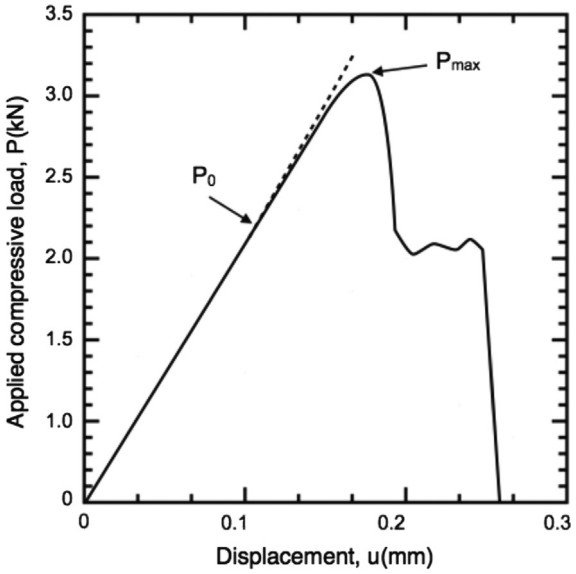

Fig. 4. Typical load–displacement curve during the test under mode I loading.

Applied load was recorded using a data collecting system (NR-500, Keyence Corp., Osaka, Japan) with a sampling rate of 50 ms, thereafter, transferred to a computer for further analysis. Micro-fracture evolution process near notch tip during the test was directly obtained using a high resolution CCD camera (VH-Z100UR, KEYENECE Corp., Osaka, Japan). After the tests, crack path at a flat surface of the specimen was observed by optical microscopy (Axioplan2 imaging, Carl Zeiss Corp., Jene, Germany) and scanning electron microscopy, SEM (TM3000, Hitachi High-Technologies Corp., Tokyo, Japan).

3. Results and discussion

Fig. 4 shows a typical example of compressive load (P)–displacement (u) relation during fracture test of a Brazilian disk specimen with a notch. The composite exhibits a linear behavior initially; however, it deviates from the initial linear relation when the applied compressive load reaches P_0. Thereafter, the relation shows a nonlinear behavior with the increase of applied compressive load up to the maximum load (P_{max}). No pop-in like behavior is observed near the transition from linear to nonlinear behavior. At the maximum load, unstable crack propagation takes place from both sides of notch tips. Fig. 5(a) and (b) shows a typical example of the micro-crack formation near a notch tip at applied load P_0 (Fig. 5(a)) and optical micrograph of notch tip in the same area before test (Fig. 5(b)), respectively. The parallel cracks are formed perpendicular to loading direction with a typical spacing of 200–650 μm. The origin of micro-crack is probably residual stress in the composite; however, more detailed analysis is needed to understand this behavior. The micro-cracks in the SiC phase are arrested when they propagate nearly perpendicular to the SCF/SiC mini-composite as shown

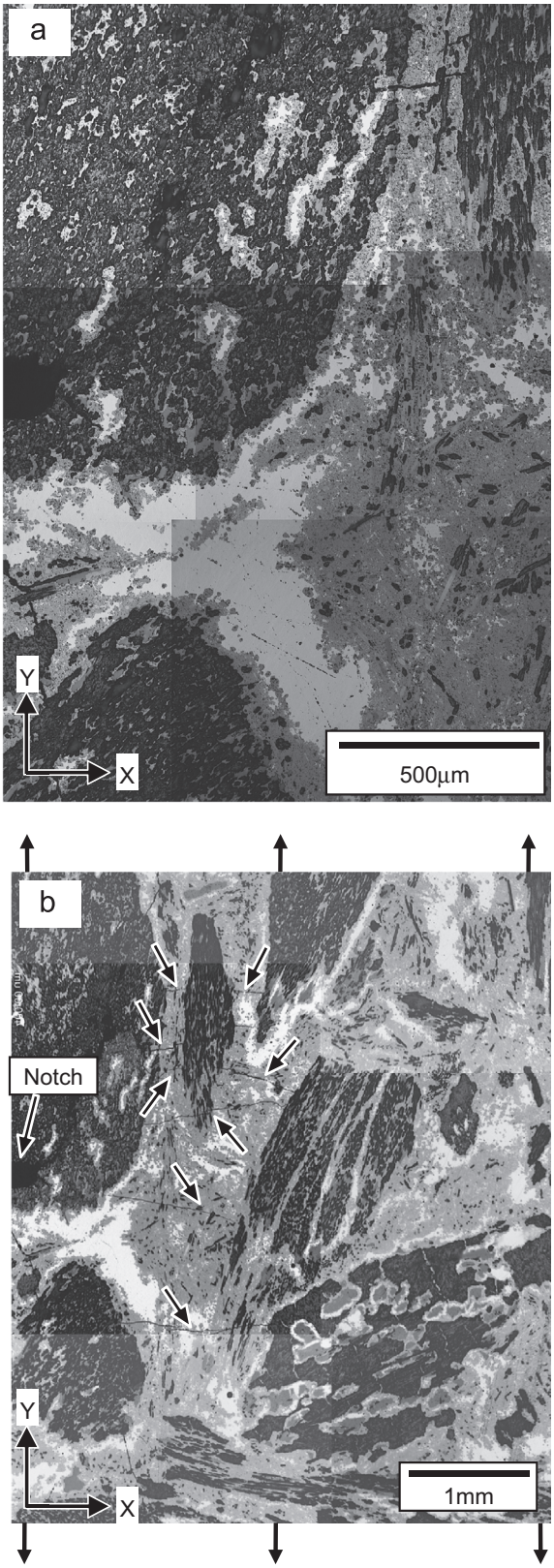

Fig. 5. Typical examples of damage evolution behavior at the starting of non-linear load–displacement curve. Arrows indicate microcracks.

in Fig. 6. This crack arrest process is a major source to help evolution of stable micro-damage zone ahead of notch tip. However, when the difference of the angle between crack

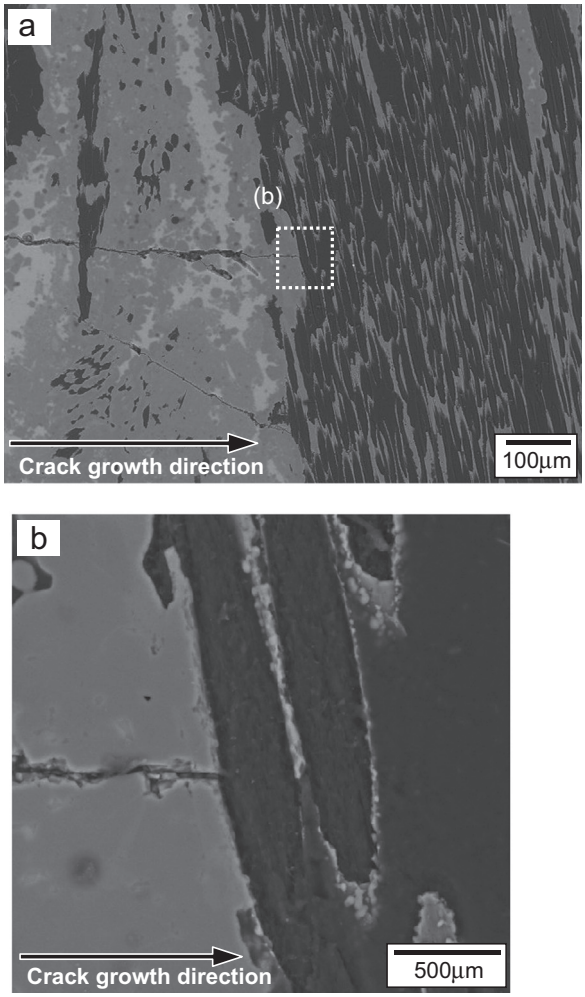

Fig. 6. Typical examples of crack arrest action at the SCF/SiC mini-composite: (a) entire view and (b) detail of (b).

propagation direction and fiber axis in the SCF/SiC mini-composite is small (typically smaller than 30°), the crack propagates easily along the fiber axis without crack arrester action (Fig. 7(a)). Observation suggests that the cracked region spreads to a circular area with a diameter of 1.8–2.3 mm ahead of notch tip. This spread of the damage zone is independent of the tested specimen although scattering within ± 0.25 mm for both the X and Y directions exists.

Unstable crack propagation takes place at the maximum load. Therefore, mode I fracture toughness of the composite, K_{Ic}, is obtained from the maximum load, P_{max}. The fracture toughness is calculated from [10];

$$K_{Ic} = \frac{P_{max}\sqrt{\pi a_0}}{\pi R t} Y_I\left(\frac{a_0}{R}, \theta\right), \quad (1)$$

where a_0 is the notch depth, and θ is the relative notch angle to loading direction. $Y_I(a_0/R, \theta)$ is the shape factor as a function of a_0/R and θ. For mode I loading condition (θ=0°), $Y_I(a_0/R, \theta)$ depends on a_0/R and is given by [10],

$$Y_I(0.5, 0) \approx 1.39. \quad (2)$$

From five tested specimens, measured fracture toughness values are listed in Table 2. It is clear that the composite has a

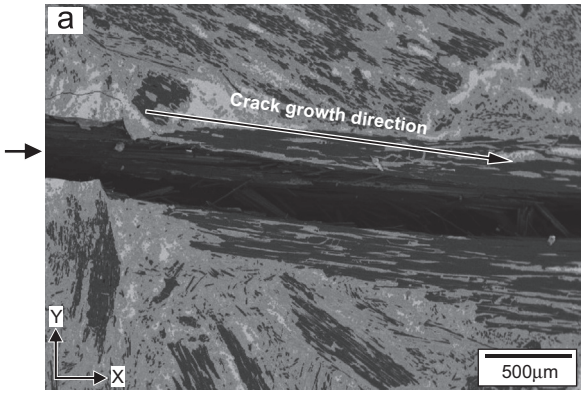

Fig. 7. Typical examples of crack propagation through SCF/SiC mini-composite.

Table 2
Measured fracture toughness of SCF/SiC composite.

Specimen	P_{max} (kN)	Fracture toughness, k_{Ic} (MPa$\sqrt{m}$)
1	2952.8	3.5
2	3055.8	3.6
3	3193.2	3.8
4	3346.6	3.9
5	3520.0	4.1

low toughness ranging from 3.5to4.1 $MPa\sqrt{m}$, which is comparable with those of monolithic ceramics, e.g., monolithic SiC (3.0–4.0 $MPa\sqrt{m}$) [11], monolithic Si (0.8–1.0 $MPa\sqrt{m}$) [11,12]. The fracture toughness range is also comparable with that of Si/SiC composite fabricated from wood precursors (2.0–2.6 $MPa\sqrt{m}$) [8,9].

In the present study, notch tip is not so sharp as a natural crack; therefore, the average stress criterion is considered to predict the fracture toughness. A similar criterion explains fracture toughness of round notch tip specimen [13,14]. The average stress criterion assumes that failure will occur when the average stress ahead of notch tip over small fixed distance, χ_D, reaches the tensile strength, $\boldsymbol{\sigma}_F$ of the SCF/SiC composite (Fig. 8). The condition is given by [13]

$$\boldsymbol{\sigma}_F = \frac{1}{\chi_D}\int_{a_0}^{a_0+\chi_D} \boldsymbol{\sigma}_y(X, 0)dX. \quad (3)$$

where $\boldsymbol{\sigma}_y(X, 0)$ is the stress in front of notch tip.

Assuming that onset of the unstable crack growth occurs when tensile stress ahead of notch tip at distance χ_D reaches a constant critical stress $\boldsymbol{\sigma}_F$, the fracture toughness is given by [13]

$$K_{Ic} \approx \boldsymbol{\sigma}_F \sqrt{\frac{\pi\chi_D}{2}}\, Y_I\left(\frac{a_0}{R}, 0\right) \quad (4)$$

Eq. (4) is generally considered to be quite accurate for $(a_0/10) \geq \chi_D$ [13]. Assuming that the critical stress is the same as tensile fracture strength of the composite ($\sigma_F \sim 45$ MPa [12]) used in this study, characteristic distance is equal to observed

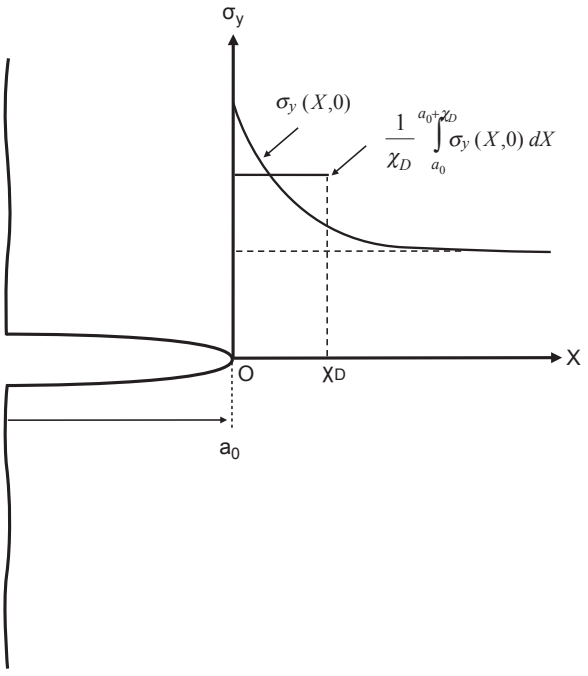

Fig. 8. Schematic drawing of stress distribution in front of notch tip.

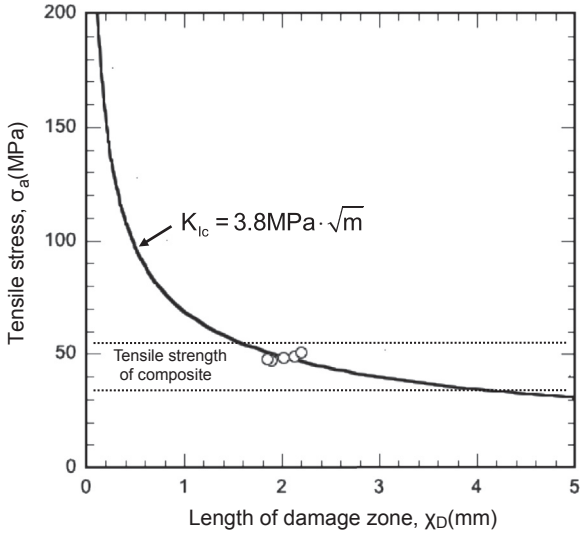

Fig. 9. Relationship between tensile stress and length of damage zone. Solid line is estimated fracture stress using Eq. (4) with $K_{Ic}=3.8K_{Ic}=3.8\,MPa\sqrt{m}$. The tensile strength range is experimental result [15].

damage zone size ($\chi_D \sim 2.0$ mm), and $Y_I(a_0/R,0)\approx 1.39$ [10], fracture toughness is estimated at $\sim 3.5\,MPa\sqrt{m}$, which is very close to the measured fracture toughness of the composite. Fig. 9 shows plots of the measured damage zone size χ_D and fracture toughness of the composite. Estimated fracture toughness vs. damage zone size relations using $K_{Ic}=3.8\,MPa\sqrt{m}$ are also presented in the figure. It is clear that experimentally obtained fracture toughness is well explained by the average stress criterion. This agreement confirms that this criterion is adaptable for the present SCF/SiC composite.

The agreement also suggests that the fracture toughness can be estimated using continuum mechanics approach although the CF/SiC composite is a heterogeneous material. However, more detailed studies are needed to further investigate the effect of heterogeneous microstructure on the fracture toughness of the present composite.

4. Conclusions

Mode I fracture toughness of SCF/SiC composite fabricated by MI process has been measured using a Brazilian disk specimen. The following results are obtained.

The fracture toughness of the composite is ~ 3.5–$4.1\,MPa\sqrt{m}$, which is the same level as those of monolithic engineering ceramics.

(1) The fracture toughness is explained by average stress criterion, $K_{Ic}\approx\sigma_D\sqrt{\pi\chi_D/2}$, using tensile strength of the composite (σ_F) and observed damage zone size (χ_D) ahead of notch tip just before unstable fracture.
(2) Within the damage zone, most of the micro-fractures occur in SiC phase. The micro-fracture is arrested by the SCF/SiC mini-composite. This arrest behavior helps evolution of micro-fracture in the composite.

References

[1] W. Krenkel, Carbon fiber reinforced silicon carbide composite(C/SiC,C/C–SiC), in: P.N. Bansal (Ed.), Handbook of Ceramic Composites, Kluwer Academic Publishers, Luwer, 2005, pp. 117–148.
[2] W. Krenkel, Ceramic Matrix Composites, Wiley-VCH, Weinheim, 2008.
[3] W. Krenkel, B. Heidenreich, R. Renz, C/C–SiC composites for advanced friction systems, Advanced Engineering Materials 4 (2002) 427–436.
[4] W. Krenkel, Carbon fiber reinforced CMC for high-performance structures, International Journal of Applied Ceramic Technology 1 (2004) 188–200.
[5] W. Krenkel, F. Berndt, C/C–SiC composites for space applications and advanced friction systems, Materials Science and Engineering A 412 (2005) 177–181.
[6] J.A. Roether, A.R. Boccaccini, Dispersion-reinforced glass and glass–ceramic matrix composites, in: P.N. Bansal (Ed.), Handbook of Ceramic Composites, Kluwer Academic publishers, Luwer, 2005, pp. 485–509.
[7] R. Warren, Ceramic–Matrix Composites, Blackie and Son, Glasgow, 1992.
[8] M. Singh, J.A. Salem, Mechanical properties and microstructure of biomorphic silicon carbide ceramics fabricated from wood precursors, Journal of the European Ceramic Society 22 (2002) 2709–2717.
[9] M. Singh, D.R. Behrendt, Reactive melt infiltration of silicon–niobium alloys in microporous carbons, Journal of Materials Research 9 (1994) 1701–1708.
[10] C. Atkinson, R.E. Smelser, J. Sanchez, Combined mode fracture via the cracked Brazilian disk test, International Journal of Fracture 18 (1982) 4.
[11] R.W. Rice, Mechanical Properties of Ceramics and Composites: Grain and Particle Effects, Marcel Dekker Inc., New York, 2000.
[12] C.P. Chen, M.H. Leipold, Fracture toughness of silicon, American Ceramic Society Bulletin 59 (1980) 469–472.
[13] J.M. Whitney, R.J. Nuismer, Stress fracture criteria for laminated composites containing stress concentrations, Journal of Computational Materials Science 8 (1974) 253–265.
[14] B.G. Agarwal, L.J. Broutmann, Analysis and Performance of Fiber Composites, 2nd ed., Wiley, New York, 1990.
[15] R. Inoue, J.M. Yang, H. Kakisawa, Y. Kagawa, unpublished research.